THE ASTROPHYSICAL JOURNAL, 283:L31–L35, 1984 August 15

THE DISTRIBUTION OF CO IN THE GALAXY FOR LONGITUDES 294° TO 86°

B. J. ROBINSON, R. N. MANCHESTER, AND J. B. WHITEOAK
Division of Radiophysics, CSIRO, Sydney
D. B. SANDERS, N. Z. SCOVILLE, AND D. P. CLEMENS
Five College Radio Astronomy Observatory
W. H. MCCUTCHEON
University of British Columbia
AND
P. M. SOLOMON
State University of New York at Stony Brook
Received 1983 December 21; accepted 1984 April 16

ABSTRACT

Observations of 115 GHz ($J = 1$–0) emission from the CO molecule for the southern galactic plane from longitude 294° to the galactic center are compared with northern galactic plane observations to longitude 86°. The longitude distribution of integrated emission is similar in the two hemispheres exhibiting broad peaks centered at about $l = \pm 25°$; the strong galactic center feature is confined to $l = \pm 2°$. The computed radial distribution of CO emissivity averaged over both hemispheres has a peak value of 12 K km s^{-1} kpc^{-1} at galactocentric radius $R = 0.5\ R_\odot$, which is 3–4 times that at $R = 0.2$ and 0.9 $R_\odot$. In the south the distribution has an approximately constant CO emissivity between 0.25 and 0.85 $R_\odot$; in the north it is sharply peaked between 0.45 and 0.65 $R_\odot$. The integrated CO emissivity in the south is about 20% larger than that in the north. Factors of 1.5–2.5 difference in the north and south emissivities at $R = 0.2$, 0.5, and 0.8 $R_\odot$ may be due to spiral arms or ring segments.

Subject headings: galaxies: Milky Way — galaxies: structure — interstellar: matter — interstellar: molecules

I. INTRODUCTION

CO is the most abundant molecule which can be readily detected at radio wavelengths. The lowest rotational transition at 115 GHz is an acknowledged primary tracer of H_2 in giant molecular clouds (GMC). The close association found between regions of active star formation (e.g., H II regions) and GMC throughout the Galaxy suggests that CO might be a good indicator of spiral structure.

In this *Letter* we give the first complete calibrated map of CO ($J = 1$–0) emission for the inner Galaxy. A well-sampled survey of CO emission in the southern hemisphere from $l = 294°$–358° and $l = 1.°3$–13° at $b = 0°$ using the 4 m telescope of CSIRO, Division of Radiophysics (Robinson, McCutcheon, and Whiteoak 1982; Robinson *et al.* 1983) is combined with data taken from an extensive northern survey ($l = 358°$–86°) carried out using the 14 m telescope at the Five College Radio Astronomy Observatory (FCRAO).[1]

Early published northern disk surveys, both with the same telescope and different telescopes, often differed in their calibration, which, if not accounted for, could lead to significant errors in estimating the amount of molecular gas in the Galaxy. Since there is now a general consensus concerning the corrected temperature scales (T_R^*—for definition see Kutner and Ulich 1981) in use at northern telescopes, it is important to present the new southern data properly calibrated against the northern data in order to accurately compute the total amount of galactic CO emission and to quantify the large-scale azimuthal variations of emission across the disk. Our complete map uses data from both hemispheres to derive a global average radial distribution of molecular gas out to $R_\odot$. The molecular cloud ring seen in earlier northern surveys by Scoville and Solomon (1975), Burton *et al.* (1975), and Cohen and Thaddeus (1977) remains the dominant feature in the galactic distribution, but differences in the width of the ring between north and south could be due to the effects of spiral arms.

II. TELESCOPES AND CALIBRATION

The beamwidths of the 4 m and 14 m telescopes at 115 GHz are 2.′7 and 50″, respectively; for both surveys the sampling interval was 3′. At intervals of 9′ in longitude, sets of nine observations at l, $l \pm 3'$, $b = 0°$, $\pm 3'$ were averaged to an effective spatial resolution of 9′ and a spectral resolution of 1 km s^{-1}. Further details of the observing procedures are given by Robinson, McCutcheon, and Whiteoak (1982) and Sanders (1983).

Considerable care was taken to calibrate the two surveys. The FCRAO scale of T_R^* was established by using observations of the Moon to correct for forward scattering and spillover, and it has been compared with scales used for

[1]The Five College Radio Astronomy Observatory is operated with the permission of the Commonwealth of Massachusetts under grant AST82-12252 from the National Science Foundation.

galactic plane CO surveys from NRAO (1.1 beam), BTL (1.7 beam), and GISS (8′ beam) using $\int T_R^* \, dv$ (where v is radial velocity) as the basis for comparison (Sanders, Solomon, and Scoville 1984). Values for $\int T_R^* \, dv$ versus longitude from each telescope are remarkably similar over the entire first galactic quadrant. The intensity scale for the southern 4 m observations was established by comparison of spectra in the region of overlap of the two surveys and at several points along the galactic plane in the longitude range 14°–30° where additional observations were made using the 4 m telescope.

III. RESULTS

a) Distribution of Integrated Emission

Figure 1 shows the calibrated CO emission integrated over all velocities, $\int T_R^* \, dv$, as a function of longitude between 294° and 66°. The distribution shows a general symmetry about the galactic center direction with broad maxima centered at about $l = \pm 25°$. There are significant differences in detail, however; for example, the strong features around $l = 340°$ and 315° have no counterparts in the north. The nuclear CO emission is confined to a sharp spike within 2° of the galactic center direction. Also shown in the figure are the results of a northern far-infrared survey (FIR) made by Boisse *et al.* (1981) with a resolution of 1°, and the γ-ray emission (70 MeV–5 GeV) observed with the 1°–5° beam of the *COS B* satellite (Mayer-Hasselwander *et al.* 1982). The three maps are similar in general appearance: all have a broad maximum within 40° of the galactic center. Correspondence of individual features (e.g., at $l = 0°$, 24°, and 30°) can be noted in the CO and FIR distributions, but such features are not so obvious in the γ-ray distribution. Notably, the large peak at the galactic center is absent from the γ-ray data. The γ-ray data have been used to indirectly estimate molecular content in the inner Galaxy (e.g., Lebrun *et al.* 1983); however, Figure 1 clearly shows that the molecular features are washed out by the large γ-ray beam.

b) Longitude-Velocity Distribution

The CO emission observed from the northern and southern hemispheres is shown in the longitude-velocity plane in Figure 2. The intensities are represented by a pseudologarithmic gray scale in Figure 2 and false color on Figure 3 (Plate L2). CO is present at predominantly negative velocities for $300° < l < 358°$, and at positive velocities for $3° < l < 80°$, indicating that the CO emission is found mainly at $R < R_\odot$. Most of the CO emission arises from the annulus 0.3 $R_\odot$ to 0.85 $R_\odot$ in the south and 0.45 $R_\odot$ to 0.85 $R_\odot$ in the north. The emission that is detected for $R > R_\odot$ is weak and patchy. The wide spread of velocities between $357° < l < 3°$ is associated with the galactic center where the rotational velocities and noncircular radial velocities reach ~ 250 km s^{-1} and 150 km s^{-1}, respectively.

One of the most intriguing questions that can be addressed by our survey concerns the delineation of spiral arms. For gas moving in circular orbits, the *l-V* track of a spiral arm in the inner galaxy will be a loop or bow, knotted at $l = 0°$, $V = 0$ km s^{-1}, and running diagonally across the *l-V* plane (see examples in Robinson *et al.* 1983). Thus the most direct approach for finding spiral arms is to search the longitude-velocity diagram for patterns matching the predicted form.

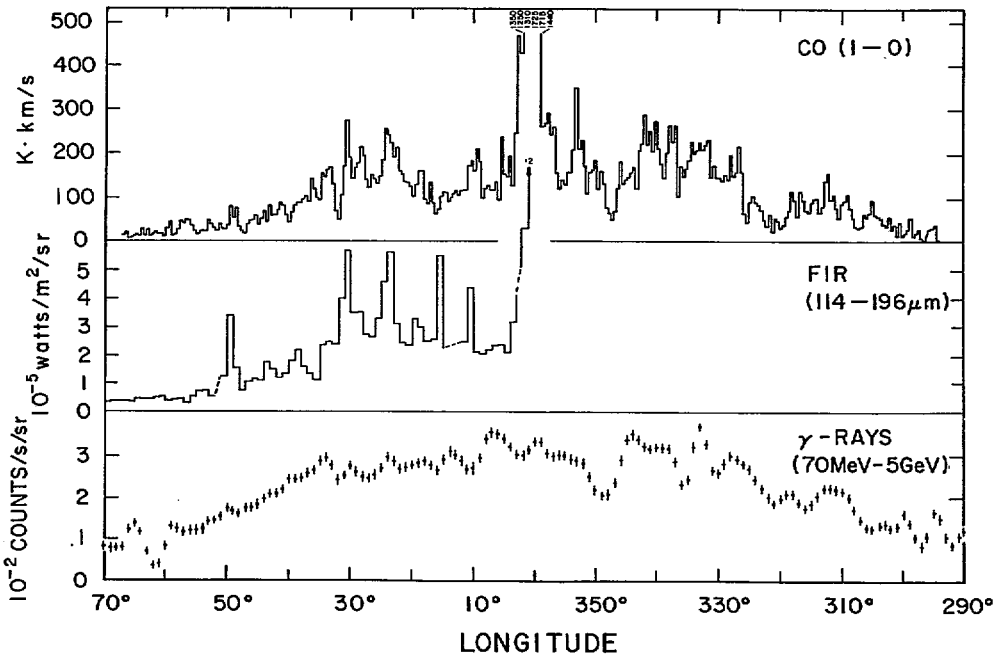

FIG. 1.—The longitude distribution of CO emission near $b = 0°$, with an effective angular resolution of 9′ binned in 0.°45 bins. Also shown are the distribution of FIR (114–196 μm wavelength) at 1° resolution (*center panel*) and the γ-ray emission (70 MeV–5 GeV) observed with the 1°–5° beam of the *COS B* satellite (*bottom panel*).

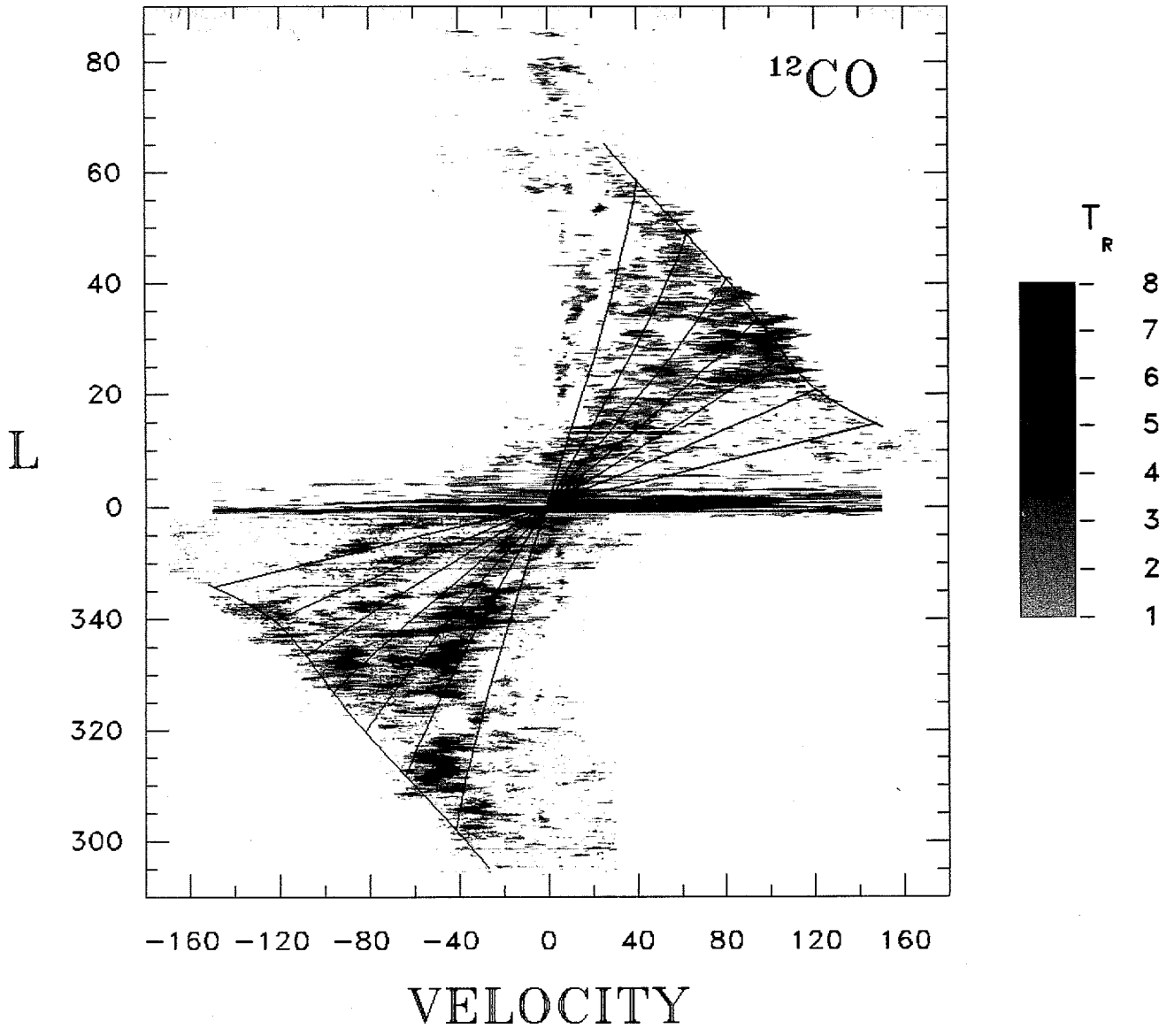

FIG. 2.—The longitude-velocity distribution of CO emission as observed by CSIRO ($294° \leq l \leq 358°$) and FCRAO ($358° \leq l \leq 86°$). The effective spatial and velocity resolutions are 9′ and 1 km s^{-1}, respectively. The intensities are represented by a gray scale in units of T_R^* with a saturation level of 6 K and a lower cutoff at 1.0 K. Superposed lines of constant galactocentric radius at 0.1 $R_\odot$ intervals between 0.25 $R_\odot$ and 0.85 $R_\odot$ and the terminal velocity were computed using the H I galactic rotation model of Burton and Gordon (1978).

Two noticeable linear features in Figure 2 are those at (1) $l = 20°$–$40°$, $V = 10$ km s^{-1}, and (2) extending from $l = 340°$, $V = -140$ km s^{-1} to $l = 10°$, $V = -15$ km s^{-1}. The former is a local feature commonly referred to as the "local arm" which can be traced for only a few hundred parsecs but extends far in longitude because of its proximity; it therefore may not be a galactic scale spiral arm. The latter is the 3 kpc "expanding" arm (cf. Bania 1977); its velocity of -53 km s^{-1} at $l = 0°$ reflects its expansion away from the galactic center.

In the remainder of the l-V plane, the clumpiness of the CO emission precludes the delineation of any continuous spiral arm patterns. There are no other clear loops matching a theoretical spiral arm. Here one must resort to other criteria indicative of large-scale segregation such as the appearance of gaps in the emission along the terminal velocity line or voids and concentrations in the l-V plane.

There are two major concentrations of emission along the northern terminus at $l = 30°$ and $l = 50°$. In the south, major peaks near the terminal velocity curve occur at $l = 309°$ and $l = 327°$. They are separated by a clear void at $l \approx 320°$. If these southern concentrations represent spiral arms tangential to the line of sight, then their galactocentric radii are 0.78 $R_\odot$ and 0.55 $R_\odot$ for the 309° and 327° features, respectively.

c) *Radial Distribution of CO Emissivity*

Figure 4*a* shows the radial distribution of CO emissivity, J, at $b = 0°$ separately for the northern and southern sections of

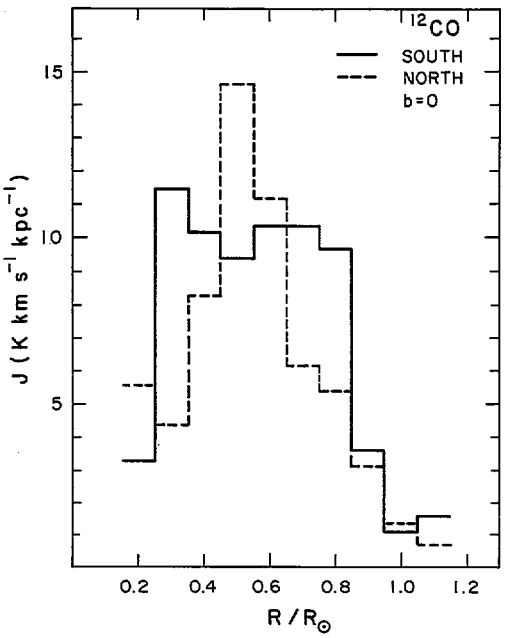

FIG. 4*a*

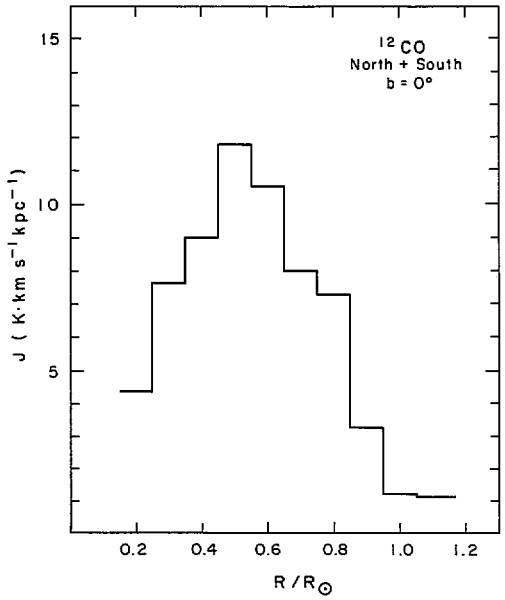

FIG. 4*b*

FIG. 4.—(*a*) The radial distribution of CO emissivity in the southern and northern hemispheres at $b = 0°$ between galactocentric radii 0.2 $R_\odot$ and $R_\odot$. (*b*) The combined (north and south) radial distribution of CO emission at $b = 0°$ for $l = 294°$–$70°$.

the galactic plane. For the northern section, data from 8° to 86° were used, and for the southern section, 294° to 352°. Excluding emission at $|l| < 8°$ eliminates the large noncircular motions associated with the galactic center emission and minimizes the effect of the expanding component of the 3 kpc arm on the computed radial distribution. In both hemispheres, the CO is concentrated in a ring between 0.3 and 0.8 $R_\odot$ with the centroid of emissivity (weighted by the area of the annulus) at 0.55 $R_\odot$. The integrated CO emissivity between 0.2 $R_\odot$ and $R_\odot$ in the south is ~ 20% larger than that in the north, suggesting the presence of somewhat more molecular gas in the southern hemisphere.

Figure 4*b* shows the radial emissivity at $b = 0°$ averaged over both hemispheres. The peak emissivity is 12 K km s^{-1} kpc^{-1} at $R = 0.5$ $R_\odot$. On the inside of the ring ($R = 0.15$–0.25 $R_\odot$) the mean emissivity is less than 30% of that at the peak of the ring, and at the solar radius the emissivity is down nearly an order of magnitude from the peak.

The detailed shape of the molecular ring in each hemisphere is different. The southern distribution is much wider (0.6 $R_\odot$ [FWHM] compared to 0.3 $R_\odot$), and it may possibly have two peaks near 0.3 and 0.7 $R_\odot$. The standard deviation of the mean J, determined at each R in Figure 4, is typically less than 5%. Significant differences between the northern and southern distributions occur in four radial bins. Within three of these (0.3, 0.5, and 0.8 $R_\odot$) the differences exceed twice the internal dispersion of 10° longitude subsets of data from the individual hemispheres. This suggests structures larger than 10° which are different between north and south.

In part, these differences result from the presence of clusters of giant molecular clouds which may contribute up to 50% of the emissivity in a given annulus. Some of the northern hemisphere excess at 0.5 $R_\odot$ is clearly due to the great concentration of emission from $l = 22°$ to 31° near the terminal velocity ($V = 90$–100 km s^{-1}). The excess in the south around $R = 0.7$ and 0.8 $R_\odot$ can be attributed to two separate concentrations near $V = -55$ to -20 km s^{-1} from $l = 325°$ to 345°, and $l = 310°$ to 318° near the terminal velocity at $V \approx -60$ km s^{-1}. There is also a small segment from $l \approx 337°$ to 343° at $V \approx -120$ km s^{-1} which accounts for some of the $R = 0.3$ $R_\odot$ excess in the south. The differences from $R = 0.45$ to 0.85 $R_\odot$ may also reflect the presence of a trailing spiral arm from $R \approx 0.5$ $R_\odot$, $l = 22°$ to 32° in the north to $R \approx 0.7$ kpc in the south from $l = 330°$ to 340°. However, the patchy nature of the distribution makes it difficult to fully trace any global spiral pattern.

IV. CONCLUSIONS

From our combined north-south CO survey, we find:

1. The distribution of integrated CO emission near $b = 0°$ between $l = 294°$ and 66° shows a general symmetry about $l = 0°$ with broad maxima near $l = 335°$ and 25° which are consistent with a ringlike distribution. The general appearance is similar to that for FIR and γ-ray emission, but there are differences in detail.

2. The *l*-*V* distribution of CO emission shows some features that can be identified with large-scale galactic structural patterns. The most prominent are associated with the "local" arm and 3 kpc "expanding" arm. CO concentrations at $l = 309°$, 327°, 30°, and 50° at the terminal velocity, together with intervening voids of gas, are consistent with clumps of gas in spiral arms viewed tangentially in these directions.

3. The radial distributions of CO emissivity between 0.2 and 0.9 $R_\odot$ for the northern and southern hemispheres are both centered near 0.5 $R_\odot$, consistent with a molecular ring structure. The mean peak emissivity is 12 K km s^{-1} kpc^{-1}, a factor of 3 larger than at 0.2 $R_\odot$ and a factor of 4 larger than at 0.9 $R_\odot$. The shape of the two distributions differ in detail—the southern CO shows a broad plateau between 0.25 and 0.85 $R_\odot$ (or possibly two separate peaks near 0.3 and 0.7 $R_\odot$), while the northern CO has a sharper peak near 0.5 $R_\odot$. These differences may result from a trailing spiral pattern for the galactic gas.

REFERENCES

Bania, T. M. 1977, *Ap. J.*, **216**, 381.
Boisse, P., Gispert, R., Coron, N., Wijnbergen, J. J., Serra, G., Ryter, C. and Puget, J. L. 1981, *Astr. Ap.*, **94**, 265.
Burton, W. B., and Gordon, M. A. 1978, *Astr. Ap.*, **63**, 7.
Burton, W. B., Gordon, M. A., Bania, T. M., and Lockman, F. J. 1975, *Ap. J.*, **202**, 30.
Cohen, R. S., and Thaddeus, P. 1977, *Ap. J. (Letters)*, **217**, L155.
Kutner, M. L., and Ulich, B. L. 1981, *Ap. J.*, **250**, 341.
Lebrun, F., *et al.* 1983, *Ap. J.*, **274**, 231.
Mayer-Hasselwander, H. A., *et al.* 1982, *Astr. Ap.*, **105**, 164.
Robinson, B. J., McCutcheon, W. H., Manchester, R. N., and Whiteoak, J. B. 1983, in *Surveys of the Southern Galactic Plane*, ed. W. B. Burton and F. P. Israel (Dordrecht: Reidel), p. 1.
Robinson, B. J., McCutcheon, W. H., and Whiteoak, J. B. 1982, *Int. J. Infrared Millimeter Waves*, **3**, 63.
Sanders, D. B. 1983, in *Surveys of the Southern Galactic Plane*, ed. W. B. Burton and F. P. Israel (Dordrecht: Reidel), p. 127.
Sanders, D. B., Solomon, P. M., and Scoville, N. Z. 1984, *Ap. J.*, **276**, 182.
Scoville, N. Z., and Solomon, P. M. 1975, *Ap. J. (Letters)*, **199**, L105.

D. P. CLEMENS, D. B. SANDERS, and N. Z. SCOVILLE: Five College Radio Astronomy Observatory, 619 GRC Tower B, University of Massachusetts, Amherst, MA 01003

R. N. MANCHESTER, B. J. ROBINSON, and J. B. WHITEOAK: Division of Radiophysics, CSIRO, P.O. Box 76, Epping, N.S.W. 2121

W. H. MCCUTCHEON: Department of Physics, University of British Columbia, Vancouver, B.C., Canada V6T 2A6

P. M. SOLOMON: Astrophysics Program, State University of New York, Stony Brook, NY 11794

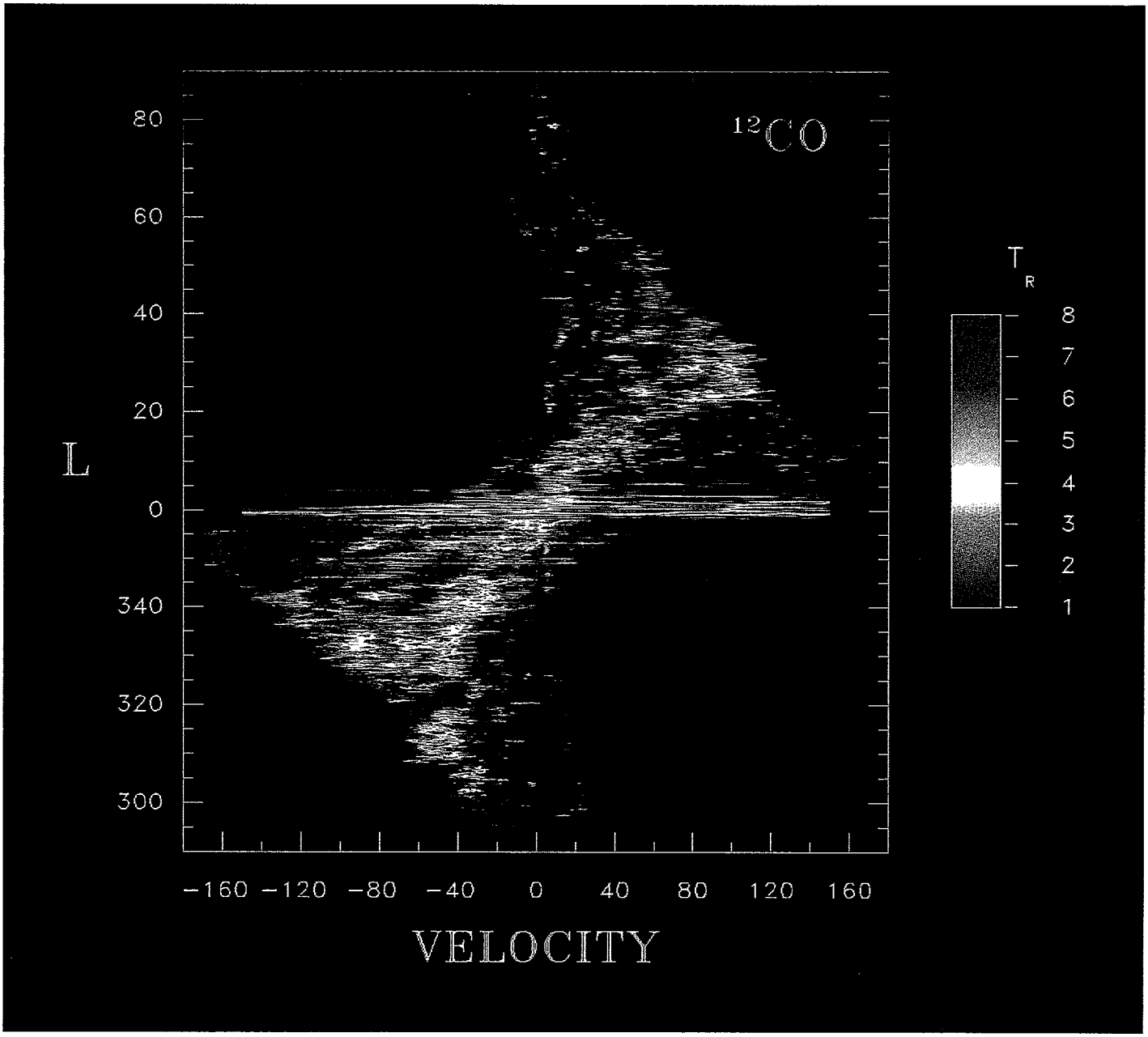

FIG. 3.—Color plate of the black and white image in Fig. 2. The intensity scale is in units of T_R^*. Saturation is at 6 K with a lower cutoff at 1.0 K. The processing of the color image was done at the University of Massachusetts Remote Sensing Center with the assistance of D. Chesley.

ROBINSON *et al.* (*see* page L32)